

# Tensile Stress–Strain and Recovery Behavior of Indian Silk Fibers and Their Structural Dependence

R. RAJKHOWA, V. B. GUPTA, V. K. KOTHARI

Department of Textile Technology, Indian Institute of Technology, Hauz Khas, New Delhi 110016, India

Received 12 May 1999; accepted 10 December 1999

**ABSTRACT:** The tensile stress–strain and recovery behavior of all the four commercial varieties of Indian silk fibers, namely Mulberry, Tasar, Eri, and Muga, have been studied along with their structures. Compared to the non-Mulberry silk fibers, Mulberry silk fiber is much finer and has crystallites of smaller size, higher molecular orientation, and a more compact overall packing of molecules. These structural differences have been shown to result in (1) the presence of a distinct yield and a yield plateau in non-Mulberry silk and their absence in Mulberry silk, and (2) relatively higher initial modulus and tenacity along with lower elongation-to-break and toughness and superior elastic recovery behavior of mulberry silk compared to non-Mulberry silk. It is also observed that fine silk fibers have a relatively more ordered and compact structure with higher orientation compared to their coarse counterparts, and this gives rise to higher initial modulus and higher strength in the finer fibers. © 2000 John Wiley & Sons, Inc. *J Appl Polym Sci* 77: 2418–2429, 2000

**Key words:** stress–strain behavior; tensile recovery; Indian silk fibers; crystallites

## INTRODUCTION

Silk is a fibrous protein and is secreted by several species of insects for building structures external to the body known as cocoons. All the four commercial varieties, namely Mulberry, Tasar, Eri, and Muga are produced in India. In the literature, a number of studies on the structure and properties of mulberry silk fiber, and to a rather limited extent on Tasar silk fiber, have been reported.<sup>1–12</sup> Some of these studies are on mechanical properties,<sup>1,7,8</sup> particularly on their load-elongation behavior and dynamic mechanical response. However, these studies on mechanical properties have mostly been made on raw Mulberry silk fibers,<sup>10</sup> although Tasar and to a more limited extent Muga silk fibers have also received some attention. However, there is hardly any detailed study

on Eri silk fiber. The present investigation on the response of the silk fibers to tensile loading and unloading has been made on all the four varieties, and an attempt has been made to correlate the stress–strain and recovery behavior of the fibers to their respective structures.

## EXPERIMENTAL

### Materials

Sufficient quantities of cross Bivoltine and Multivoltine Mulberry, Temperate Tasar (bivoltine), Muga (Multivoltine), and Eri (Multivoltine) cocoons were collected from different sources in Northeast India for the investigation.

### Methods

#### *Processing of Cocoons*

Mulberry cocoons were cooked in plain water at 90–95°C for about 15 min. Tasar and Muga co-

---

Correspondence to: V. B. Gupta.

*Journal of Applied Polymer Science*, Vol. 77, 2418–2429 (2000)  
© 2000 John Wiley & Sons, Inc.

coons were cooked in water containing 0.5% by weight of sodium carbonate with material to liquor ratio of 1 : 20 for 20 min at 95°C. Temperate Tasar cocoons were cooked in water containing 0.5% sodium carbonate and 0.5% sodium silicate with material to liquor ratio of 1 : 20 at 90°C for 30 min. Eri cocoons, being open mouthed, were not reelable. So no cooking was done for Eri cocoons. The cocoons were brushed manually in order to obtain filament end.

In the case of Eri silk, cocoons were degummed in a water bath with a material to liquor ratio (MLR) of 1 : 20, having 5% sodium carbonate and 1% nonionic wetting agent, for 3 h at 95°C. Five layers from outside to inside of the cocoons were then separated.

### Reeling

Each cocoon was reeled out using a laboratory wrap reel. While reeling, successive reeled lengths of 30 m were cut and numbered sequentially so as to identify location of these small filament segments in a cocoon during subsequent testing. Care was taken during the reeling to ensure that the filament was not stretched and properties did not change during reeling. The temperature and other conditions of reeling of different silk fibers are given below:

Mulberry: Distilled water at 40–45°C.

Muga: 0.25% Na<sub>2</sub>CO<sub>3</sub> in distilled water at 40–45°C.

Tasar: Dry reeling after cocoons were lightly pressed to remove water, while allowing them to remain moist.

After reeling, filaments were washed in distilled water to remove any residual alkali present.

### Degumming of Reeled Out Filaments

A number of reeled filaments from different cocoons of same variety were segregated depending upon fineness. Filaments were then degummed separately in groups. Degumming was carried out in small beakers placed in a Julaba, in which beakers swing in a heated water bath. The conditions of degumming were as follows:

Temperature: 90°C.

Time: 3 h.

MLR: 1 : 50.

Additives: 2 g/L sodium carbonate + 2 g/L sodium silicate + 0.25 g/L nonionic wetting agent.

The degummed samples were then treated in the following solvents in the given order to remove any residual fats.

- 8 h in methanol and diethylene ether (3 : 1).
- 24 h in cyclohexane.
- 8 h in benzene.

### Determination of Density of Degummed Silk

The density of the degummed fiber was measured using a Davenport density gradient column, which was prepared using carbon tetrachloride (density 1.599 g/cm<sup>3</sup>), and n-heptane (density 0.68 g/cm<sup>3</sup>). The column was calibrated with standard floats of known density and calibration curve of height vs density was plotted. The samples in the form of tiny round balls were allowed to settle in the column for 24 h, before taking the reading. The densities of fiber samples were determined from their respective heights in the column, through the calibration curve.

### Load-Elongation Behavior

Silk fibers of 5 cm length were first mounted on paper windows at a pretension of 0.02 gf/den. The load-elongation characteristics of these samples were then obtained on an Instron tensile tester (Model 4301) interfaced with a computer at 100%/min rate of extension in standard atmospheric conditions. From the load-elongation curves, stress-strain curves were constructed. The initial modulus, strain at failure, tenacity or breaking stress, and toughness were computed from these curves. Twenty-five tests each were carried out on both coarse and fine filaments.

### Recovery Behavior

To study the recovery behavior, the following two type of experiments were conducted on the Instron tensile tester.

*Continuous Cyclic Tests.* Instron tensile tester (Model 4301) was set to the extension cyclic mode and fiber of 5 cm length, mounted on a window with a pretension of 0.02 gf/den, was cycled from zero strain to fixed strains of 1 and 3%, respectively, at a strain rate of 4%/min for up to twenty cycles. From the cyclic loading and unloading

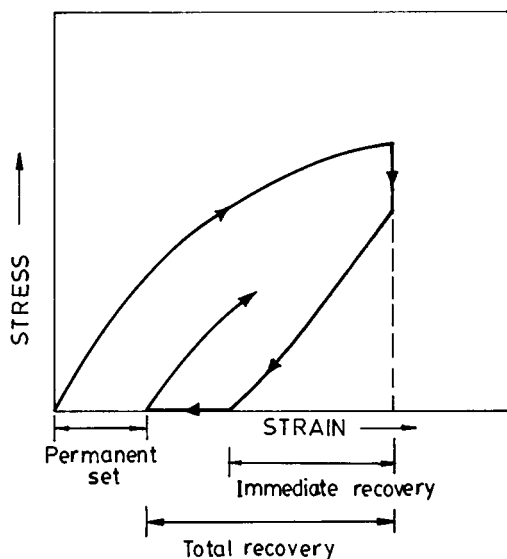


**Figure 1** Discontinuous recovery cycle and definition of terms used in the text.

curves, the percentage recovery after each cycle was estimated. Ten samples were studied for each variety and the average of the observed values has been reported. Tests were carried out only for the coarse filaments from the outer layer of the cocoons.

**Discontinuous Cyclic Tests.** The discontinuous test cycle is shown in Figure 1 and is described in the literature.<sup>13,14</sup> Fibers mounted on 5 cm paper windows with a pretension of 0.02 gf/den were extended on an Instron tensile tester (Model 1112) at a strain rate of 20%/min to a constant strain in the 3–20% range for different varieties and then held at that strain for 2 min, during which stress relaxation takes place. After this, the crosshead was returned to its original position. After 5 min, the fiber was reextended. From the plots, the 2 min percentage stress relaxation, the percentage immediate recovery, and percentage total recovery were determined, as indicated in Figure 1. Ten samples of each variety were tested. Tests were conducted on filaments collected from the outer layer of the cocoons, i.e., only coarse fibers were studied.

#### X-Ray Diffraction Studies

The silk fiber samples were cut into very small pieces of length close to the sample thickness with the help of a pair of scissors with sharp edges, taking care to avoid shearing of the sample. The

powdered sample was compressed into a rectangular slot of  $20 \times 15 \times 2$  mm size in a glass sample holder by applying 5 kg weight for 30 min on powder filled in the slot. The low resultant pressure resulted in a compact pellet, which remained stable without sagging for up to 2–3 h. The fineness of the powder and the low pressure used ensured randomness of the sample. The sample holder was then mounted on the Philips vertical powder diffractometer. The X-ray used was nickel-filtered  $\text{CuK}_\alpha$  radiation, and a curved crystal graphite monochromator was used before the detector. The sample was scanned at the rate of  $1^\circ/\text{min}$  using symmetrical reflection geometry, from  $2\theta = 10^\circ$ – $35^\circ$ .

#### Measurement of Refractive Index and Birefringence

The Beckeline method was used to measure the birefringence as the cross-section of the fibre was not circular. This method is based on measuring the parallel ( $n_{\parallel}$ ) and perpendicular ( $n_{\perp}$ ) refractive indices of the fiber on a polarizing microscope using liquid mixtures of matching refractive indices.

A range of liquid mixtures was prepared by mixing two liquids in different proportions. The liquids used for the study had the following refractive indices at  $30^\circ\text{C}$  for sodium light ( $n_D^{30}$ ):

$$\begin{aligned} \text{Paraffin liquid:} & \quad n_D^{30} = 1.482 \\ \text{Bromonaphthalene:} & \quad n_D^{30} = 1.659 \end{aligned}$$

The fiber sample was mounted on a glass slide in a straightened configuration and a drop of liquid mixture was placed on the sample. The drop was covered with a thin glass cover. With the polarizer axis parallel to the fiber axis, the sample was examined on a polarizing microscope. A pair of bright lines appears at the edges of the fiber if the refractive index of the fiber does not match the refractive index of the liquid mixture. These two lines, which are termed “Beckelines,” move toward the medium of higher refractive index when the specimen–objective distance is increased and vice versa. When the refractive indices match, Beckelines disappear. The perpendicular refractive index was similarly measured. The birefringence ( $\Delta n$ ) is given by:

$$\Delta n = n_{\parallel} - n_{\perp}$$

Twenty fiber samples taken from the coarsest and finest regions of 10 cocoons of each variety

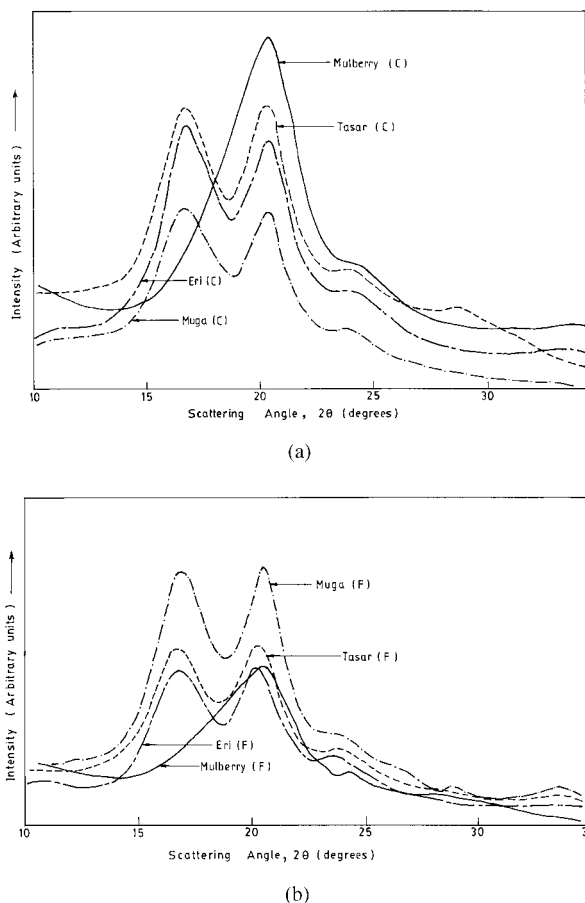


**Figure 2**  $I - 2\theta$  curves for silk fibers. (a) Coarse fibers and (b) fine fibers.

were studied and the average value has been reported as birefringence.

## RESULTS AND DISCUSSION

The main thrust of the present work was on seeking correlations between the stress-strain and recovery behavior of the Indian silk fibers with their structures, and therefore the structural data will be presented first.

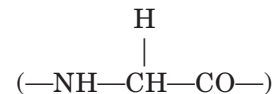
### X-Ray Diffraction Data

The  $I - 2\theta$  plots, as obtained from X-ray diffraction studies on powder samples prepared from the four Indian silk fiber varieties, are shown in Figures 2(a) and 2(b), respectively. It is noteworthy that in both cases the scattering curves for the three non-Mulberry silk fibers are, broadly speaking, of similar nature in that they all have two

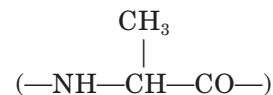
prominent peaks at  $2\theta = 16.8^\circ$  and  $21.1^\circ$  corresponding to crystalline spacings of 5.27 and 4.41 Å, respectively. The scattering curves for the coarse and fine Mulberry silk fibers, on the other hand, have only one prominent peak at  $2\theta = 21.1^\circ$ . Obviously this principal difference in X-ray diffraction data is because the crystal structures of the mulberry and non-Mulberry silk fibers are different, which is apparently due to the difference in their chemical constitutions.

Detailed studies of amino acid composition were made by Nadiger et al.<sup>15</sup> first on the silk fibroin in the four varieties of Indian silk fibers and second of the crystalline regions of silk fibers obtained by partial acid hydrolysis. Their main conclusions, which are consistent with the results obtained by Shaw and Smith,<sup>16</sup> may be summarized under the following two headings:

1. For silk fibroin:
  - (a) In Mulberry silk, glycine, alanine, and serine contribute around 85% of the total amino acid content while in non-Mulberry silk fibers, their contribution is close to 75%.
  - (b) In Mulberry silk, the glycine content is more (around 44% as opposed to 24–31% in non-Mulberry silk), while the alanine content is less (around 29% as opposed to 35–48% in non-Mulberry silk).
2. For silk hydrolysate (crystalline phase):
  - (a) In Mulberry silk, glycine and alanine are the major constituents with a detectable amount of serine. Thus the crystallites in Mulberry silk are mainly peptide units derived from glycine



and alanine



- (b) In non-Mulberry silk fibers, alanine is the major constituent with small quantities of glycine and serine. Thus the crystallites in non-Mulberry silk fibers are based predominantly on alanine units.

It will be expected that these significant differences in the chemical constitutions of mulberry

**Table I Data on Crystalline Fraction in Indian Silk Fibers**

Variety of Silk Fiber	X-Ray Crystalline Fraction	Infrared Crystalline Index
Mulberry	0.35–0.37 (Coarse) 0.42–0.43 (Fine)	0.66
Tasar	0.40	0.50
Eri	—	0.60
Muga	0.43	0.50

and non-Mulberry silk fibers will lead to important differences in molecular packing and crystalline morphology between them. It has been reported<sup>17</sup> that the crystalline density of non-Mulberry silk fibers is the same and lower than that of Mulberry silk fiber.

An accurate estimate of the crystalline fraction from the  $I - 2\theta$  plots of silk fibers involves complex procedures that limit their accuracy and was therefore not attempted. Iizuka et al.<sup>4,6</sup> have analyzed their X-ray scattering data for three of the four Indian silk varieties and the X-ray crystalline fractions in these fibers, as estimated by them, are summarized in Table I. Also included in this table are the values of crystallinity index for these fibers as estimated by Bhat and Nadiger<sup>18</sup> using infrared spectrophotometry. It is interesting to note that the higher crystalline content of Mulberry silk fiber compared to those of the non-Mulberry silk fibres, as indicated from infrared studies, is not reflected in the X-ray data. The possible reason for this difference will be briefly considered.

Tsukada et al.<sup>19</sup> made X-ray diffraction studies on Mulberry and Tasar silk fibers. Their  $I - 2\theta$  plots showed characteristics similar to the plots presented in Figures 2(a) and 2(b). A detailed analysis of their X-ray data led them to the conclusion that the fibroin molecules in Mulberry silk fiber show quite a high degree of order and orientation, but may not be as well packed as in a perfect crystalline structure. They proposed a three-phase structure for Mulberry silk. The third phase, which constituted around 30% of the fiber, had laterally ordered regions that did not form a lattice; this phase had features intermediate between the two other phases, viz., the crystalline and the amorphous phase. The Tasar fiber, on the other hand, was closer to a two-phase structure, though it also had a much smaller fraction of

intermediate phase. It would thus appear that Mulberry silk has structural characteristics of a paracrystalline fiber. Support for this observation comes from crystal size measurements, which show<sup>18</sup> that Mulberry silk fibers have smaller crystallites in the range 10–20 Å while in non-Mulberry silk they are in the 40–60 Å size range. Wide angle X-ray diffraction may not pick up structure of the order present at such a small level.

### Density Data

The density data for the coarse and fine silk fibers studied are shown in Table II. Taking the average values first, it is interesting to note that for all the non-Mulberry silk fibers, the density values are quite close but much lower than the average density value for Mulberry silk fiber. Though the chemical constitutions of these protein fibers are different, this difference in density may be taken to be indicative of greater compactness of molecular packing in Mulberry silk compared to the other silk fibers studied.

Another noteworthy point is that while in the case of non-Mulberry silk fibers, the finer fibers have higher densities, this is not the case for Mulberry silk fiber. This has been noted by other authors<sup>8,20,21</sup> also and has been attributed to the presence of a large number of small microvoids in fine Mulberry silk fiber.

It has been reported<sup>19</sup> that Mulberry silk possesses a higher degree of order and higher molecular orientation in the amorphous regions compared to Tasar silk. It has also been reported<sup>17</sup> that the density of the amorphous region in Mulberry silk is higher than that for non-Mulberry silk fibers, which are equal. All these factors con-

**Table II Density Data for the Coarse (c) and Fine (f) Fibers (the Values in Parentheses Represent the Average Values)**

Variety of Silk Fiber	Density (g/cm <sup>3</sup> )
Mulberry (c)	1.362
Mulberry (f)	1.347 (1.355)
Tasar (c)	1.300
Tasar (f)	1.320 (1.310)
Eri (c)	1.308
Eri (f)	1.320 (1.314)
Muga (c)	1.307
Muga (f)	1.308 (1.308)

**Table III Refractive Index and Birefringence Data for Silk Fibers Measured by the Beckline Method (Values in Parentheses Represent Average Values)**

Variety of Silk Fibre	$n_{\parallel}$	$n_{\perp}$	$\Delta n = n_{\parallel} - n_{\perp}$
Mulberry (c)	1.594	1.544	0.050
Mulberry (f)	1.597	1.545	0.053 (0.052)
Tasar (c)	1.562	1.521	0.041
Tasar (f)	1.564	1.526	0.038 (0.040)
Eri (c)	1.567	1.530	0.037
Eri (f)	1.567	1.530	0.037 (0.037)
Muga (c)	1.562	1.523	0.039
Muga (f)	1.563	1.523	0.040 (0.040)

tribute to the higher density of Mulberry silk fiber.

As stated earlier, the crystalline regions in silk fiber that contain fully extended chains, are made up predominantly of peptide units, with side groups  $-\text{H}$  and  $-\text{CH}_3$ . The presence of larger residues like  $\text{HO}-\text{C}_6\text{H}_4-\text{CH}_2-$  in Tyrosine are precluded in the crystalline regions. Most of the amino acid residues with bulky and polar side groups would be expected to reside in the amorphous regions of the fiber and these are more abundant in non-Mulberry silk fibers. The presence of small side groups in the amorphous regions of mulberry silk fiber permits the arrangement of the protein chains with some degree of order and orientation.

### Refractive Index and Birefringence Data

The refractive index and birefringence data for the coarse and fine silk fibers are shown in Table III. It is noteworthy that like density, the average birefringence values for non-Mulberry silk fibers are quite close and are much less than the average birefringence of Mulberry silk fiber.

In view of the differences in the chemical constitutions of the silk fibers, a direct comparison of the average birefringence values of different silk fibers in terms of molecular orientation is not entirely justified. However, an examination of the refractive indices in the parallel ( $n_{\parallel}$ ) and perpendicular ( $n_{\perp}$ ) directions is quite instructive. Mulberry silk has much higher values of  $n_{\parallel}$  and considerably higher values of  $n_{\perp}$  compared to the corresponding values for non-Mulberry silk. This is indicative of the higher orientation of molecules in the fiber. Since birefringence of a fiber has

contributions from both the crystalline and amorphous phases, the substantially higher birefringence value of Mulberry silk suggests higher orientation of both the phases. However, as the intrinsic birefringence values of the two phases are not available, the contributions of the two phases cannot be separately estimated. It is worth emphasizing that oriented molecules result in a more compact structure. Thus the optical birefringence data, combined with density and X-ray diffraction data presented earlier, suggests that overall molecular packing is much more compact in Mulberry silk fibers.

Another noteworthy observation is that though the fine Mulberry silk fiber has a lower density than its coarse counterpart, the molecular orientation is relatively higher in the fine fiber. This is consistent with the statement made earlier that the lower density of fine Mulberry fiber is due to the presence of a large number of small microvoids.

### Stress-Strain Behavior

#### *General Characteristics of the Stress-Strain Curves*

The average tensile stress-strain curves for the four Indian silk fibers (both coarse and fine), obtained at a strain rate of 100%/min, are shown in Figure 3. Some general comments on these curves can be made. Mulberry silk stands out as a fiber with high modulus, high strength and low elongation-at-break in comparison to non-Mulberry silk fibres. Another noteworthy difference is that while non-Mulberry silk fibers show a distinct yield with a yield plateau and a strain-hardening region, Mulberry silk does not show these features. These mechanical parameters will be discussed briefly in this section followed by a critical assessment of their structural dependence.

#### *The Yield Process and its Structural Dependence*

A sharp yield point at 2.5–3.5% strain can be seen for all non-Mulberry silk fibers and is more prominent in coarse fibers in all cases. The extension at almost constant load or slightly increasing load following the yield point gives rise to the yield plateau that continues up to 5–8% strain depending upon the variety and fineness. A strain-hardening region of higher modulus follows this region. A distinct yield point is not seen for Mulberry silk though in this case also the coarse fiber does show a yield point. In the case of fine Mulberry silk fiber, a slight reduction in modulus is

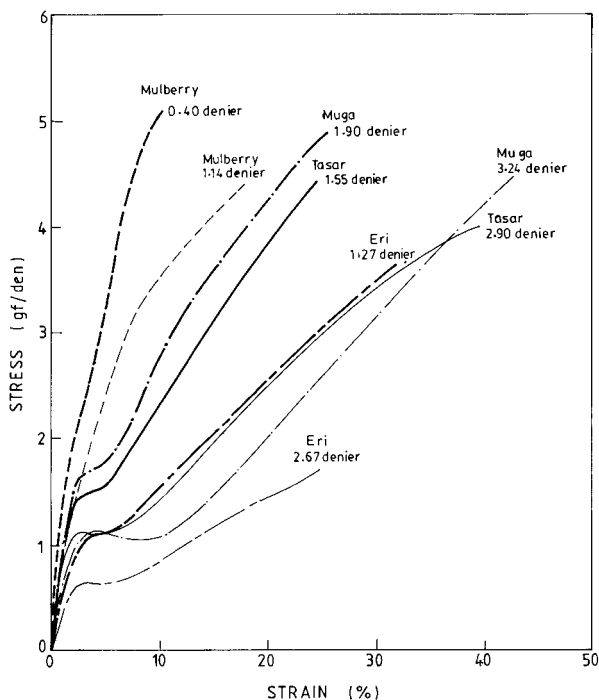


**Figure 3** Stress-strain behavior of silk fibers studied.

observed with increasing extension. However, it was observed that when the fine Mulberry fiber is tested at a reduced strain rate of 20%/min, a very weak yield is observed in the load-elongation curve (Fig. 4) but there is no plateau. A second yield point, which is not very sharp, is seen at a higher strain in all varieties in the load-elongation curves obtained at a low strain rate. In Figure 5, the second yield point for Muga silk fiber tested at a strain rate of 20%/min can be seen quite clearly.

To understand the structural basis of yield in oriented fibers, it may be recalled that during a tensile test, the amorphous phase, being more compliant than the crystalline phase, is the first to deform on application of load. The initial resistance to deformation, which is significant, arises from the interchain bonds that bind the molecules in the amorphous regions, the entanglements between the chains present in the amorphous regions, the constraints arising from the rigid crystallites between which the amorphous regions are sandwiched, and the restriction to free movement in the laterally ordered oriented amorphous regions. After the initial deformation, with increasing load and continued extension, the interchain bonds in the amorphous region of silk can break<sup>22</sup> and make it easier for the molecular chains to

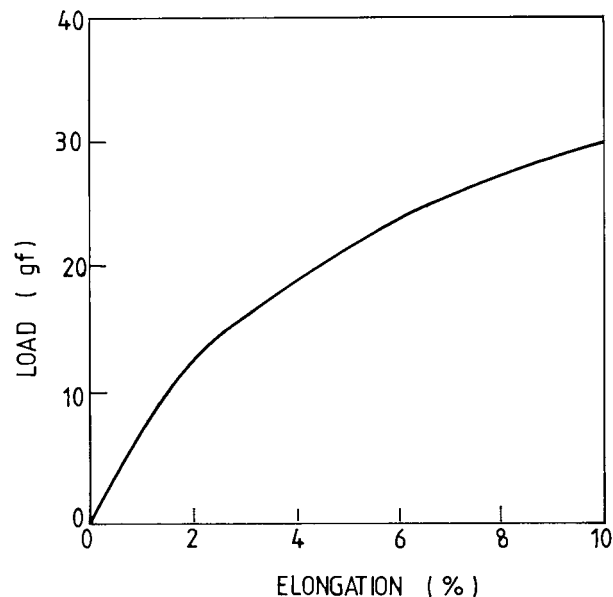


**Figure 4** Load-elongation curve of Mulberry silk fiber at a strain rate of 20%/min for elongation up to 10%.

extend. Of course, this will largely depend on the state of amorphous orientation. If the amorphous regions have randomly arranged chains, as is the case for non-Mulberry silk fibers, they can continue to extend at almost a constant load or with slight increase in load, and give rise to a distinct yield and the yield plateau. Since the molecular

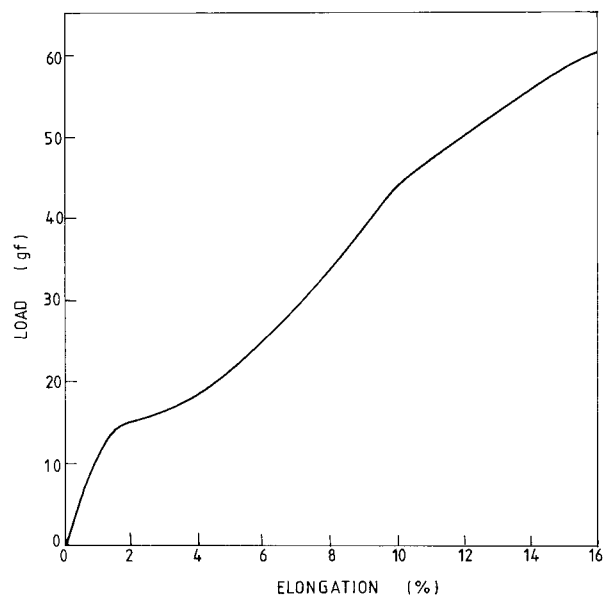


**Figure 5** Load-elongation curve of Muga silk fiber at a strain rate of 20%/min for elongation up to 16%.

**Table IV Tensile Properties of Different Varieties of Silk Fibers (The Values in Parentheses Are Percentage Coefficient of Variation)**

Property	Silk Fiber							
	Mulberry		Tasar		Eri		Muga	
	Coarse (1.14 denier)	Fine (0.40 denier)	Coarse (2.90 denier)	Fine (1.55 denier)	Coarse (2.67 denier)	Fine (1.27 denier)	Coarse (3.24 denier)	Fine (1.90 denier)
Initial modulus (gf/den)	87.50 (18.91)	120.9 (20.1)	66.68 (16.33)	69.82 (19.96)	29.38 (24.62)	31.13 (22.40)	65.55 (12.58)	73.73 (13.36)
Tenacity (gf/den)	4.43 (7.07)	5.17 (11.48)	3.92 (9.93)	4.47 (10.54)	1.87 (29.35)	3.47 (23.5)	4.57 (7.1)	4.91 (10.01)
Breaking strain (%)	17.25 (15.07)	10.56 (15.25)	39.46 (15.51)	25.91 (25.41)	24.02 (35.7)	27.45 (30.6)	40.68 (13.66)	26.4 (14.07)
Toughness (gf/den)	0.51 (20.59)	0.33 (25.96)	0.98 (26.97)	0.69 (25.55)	0.30 (63.4)	0.62 (50.5)	1.06 (14.90)	0.83 (25.29)

chains in the amorphous regions of Mulberry silk fiber have relatively higher orientation, a distinct yield or a yield plateau is not seen. However, as stated earlier, with increasing extension a reduction in modulus is obtained at higher extensions.

The appearance of a weak yield point at low strain rates in Mulberry silk may be explained as follows. As strain rate decreases, the molecular chains have more time to deform and a greater number of chains can participate in the deformation process. As stated earlier, after initial deformation, in which the modulus is quite high, some interchain bonds may break and permit the chains to deform more easily, giving a lower modulus. Stress relaxation studies on Indian silk fibers reported in another publication<sup>23</sup> showed that the stress relaxation rate for Mulberry silk is lower than the rates observed for non-Mulberry silk fibers. Thus while the elastic component was more prominent in Mulberry silk, the non-Mulberry silk fibers had a greater degree of viscoelastic component. It would thus appear that at lower strain rates, the viscoelastic effects become more marked in Mulberry silk also and this can lead to a weak yield being observed in the stress-strain curve.

The phenomenon of second yield has been widely observed in manufactured fibers (see, for example, ref. 24) like high density poly(ethylene) and poly(ethylene terephthalate) fibers, which has been attributed to the structural changes in the crystalline phase. It is likely that at higher extensions at which the yield is observed in silk fibers, the loads will be taken up by the crystal-

lites, which can undergo some structural changes on further extension. However, in the absence of reported data on this aspect, no further comments can be made on the physical mechanisms responsible for the second yield in silk fibers.

#### ***Other Mechanical Parameters Derived from Stress-Strain Curves and Their Structural Dependence***

The values of initial modulus, as estimated from the slope of the initial part of the stress-strain curve, breaking stress or tenacity, breaking strain and toughness, as obtained from the area below the stress-strain curve, are shown in Table IV. The following noteworthy observations may be made:

- Eri Silk fiber, which comes from an open-mouthed cocoon and therefore is not reelable, shows maximum coefficient of variation in all mechanical properties. Interestingly, the fiber fineness in a particular layer of the cocoon was found to be highly variable for Eri silk.
- Compared to their coarse counterparts, the fine filaments are stiffer and stronger in all the four silk fiber varieties. Also, percentage strain at break is generally lower in fine filament, with Eri silk being an exception.
- Mulberry silk fibers are the stiffest and the strongest while Eri silk fibers have the lowest moduli and lowest strength, with Muga and Tasar having intermediate values.



- Muga silk fiber has the highest toughness followed by that of Tasar silk, while the toughness is low for Mulberry and Eri silk fibers.

Based on the structural data presented earlier, a reasonably clear picture emerges as far as the structural dependence of mechanical properties in these four varieties of silk is concerned, and some important aspects of this will now be highlighted.

To begin with, an examination of the data given in Table IV shows that the modulus and strength values of most of the silk fibers are quite high, and among the natural fibers, silk may be considered to be outstanding as far as these properties are concerned. Coupled with a reasonably high breaking extension, the high modulus and high strength result in high work-to-rupture or toughness. In general, this good combination of properties arises because silk has fairly high crystallinity and high orientation, and its morphology is relatively more simple and close to that of manufactured fibers. However, among the four silk fibers studied, there are substantial differences in structure and these introduce differences in mechanical properties. Some of these aspects will now be considered.

The degree of crystallinity is quite high in silk fibers, though its exact measurement is difficult. The crystallites will be expected to reinforce the structure of silk. However, while the differences in crystalline content in the different fibers are not so large, the differences in orientation are quite substantial. As stated earlier, on application of load, the more compliant amorphous phase is the first to deform. It had already been argued that the presence of randomly oriented molecules in the amorphous phase of non-Mulberry silk fibers gives them their relatively higher extensibility. The relatively low extensibility of Mulberry silk correlates well with its high birefringence. The presence of side groups with interchain bonds in the amorphous regions and the laterally ordered regions in the oriented amorphous phase will restrict the free rotation of molecules, and thus lower their extensibility. The high modulus of Mulberry silk will have the same structural origin.

As extension continues, the load is progressively transferred to the crystalline regions. It is worthwhile recalling that Mulberry silk has a crystalline structure that differs from the structures of non-Mulberry silk fibers, an important

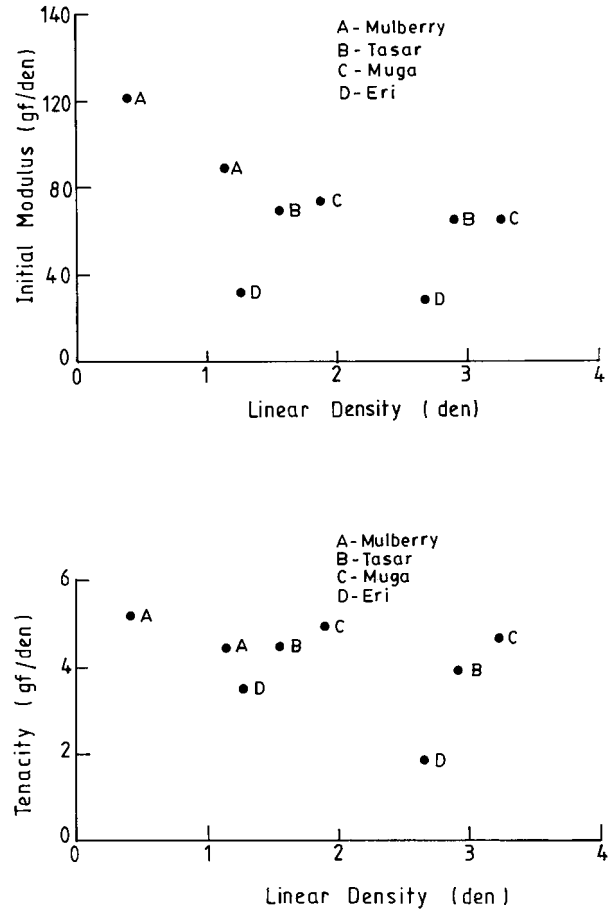


**Figure 6** Effect of fiber fineness on (a) initial modulus and (b) tenacity.

difference being that the crystal size in Mulberry silk is much smaller. Thus even if it has the same degree of crystallinity as that of other fibers, there would be a large number of small crystallites in Mulberry silk, and these will reinforce the structure more effectively than a smaller number of larger crystallites, mainly by putting greater constraints on the mobility of amorphous regions. This will contribute to the enhanced strength.

We next consider the observed higher modulus and higher tenacity of the fine fibers compared to those of their coarse counterparts. The dependence of the modulus and strength values of the four varieties of Indian silk are shown as a function of their fineness in Figures 6(a) and 6(b), respectively. If Eri silk fibers, which are reported<sup>2,20</sup> to contain large microvoids that may be responsible for its low stiffness and strength, are kept out, the correlation seems to be reasonable. It is interesting to recall that the fine fibers were seen to have higher crystallinity, higher density, and higher birefringence than their coarse counterparts.

It was shown by Meredith<sup>25</sup> that tenacity, breaking extension, and initial modulus of silk were related to fiber fineness. Meredith found that in general, the finer the silk, the higher the tenacity and the initial modulus, and the lower the breaking extension. Iizuka et al.<sup>2</sup> have shown that the tensile strength and modulus along different filament lengths from within the same cocoon and among different species correlates well with fineness. Iizuka<sup>26</sup> has demonstrated a linear relationship of static and dynamic Young's modulus and of X-ray crystallinity to fiber fineness. He showed that the finer the fiber, the higher the Young's modulus and the greater the degree of crystallinity. A correlation between crystallite orientation and fineness was also demonstrated.

### Recovery Behavior and Its Structural Dependence

The results of the continuous cyclic tests at 1 and 3% strain are presented in Figures 7(a) and 7(b), respectively. There are two points worth noting from these curves; first, at 1% strain level, the recovery is much greater than at 3% strain at corresponding cycles for all varieties, as expected. Second, while Mulberry silk fiber shows the best recovery characteristics, Muga silk fiber is seen to have poor recovery particularly at 3% strain level. This is apparently because Muga silk fiber shows a very distinct yield point below 3% strain, as is clear from Figure 5.

The results of the discontinuous cyclic tests are presented in Figures 8–11. The stress that relaxes during 2 min relaxation at a fixed strain is shown in Figure 8 as a function of applied strain and it decreases as the applied strain increases, as expected. It is noteworthy that stress relaxation is the lowest in Mulberry silk fiber. This supports the observation made earlier that Mulberry silk shows a relatively lower degree of viscoelasticity compared to other silk fibers. The immediate recovery is shown as a function of applied strain in Figure 9. It is interesting to note that the immediate recovery is the highest for Mulberry silk fiber. For both Tasar and Muga silk fibers, the recovery behavior is more complex. This can possibly be explained on the basis of their stress-strain curves (Figures 3 and 5), which show two yield points and a region of strain hardening between the first and the second yield points. The delayed recovery after 5 min is shown in Figure 10, and as expected, it decreases as the applied strain increases for all the varieties of silk fibers.

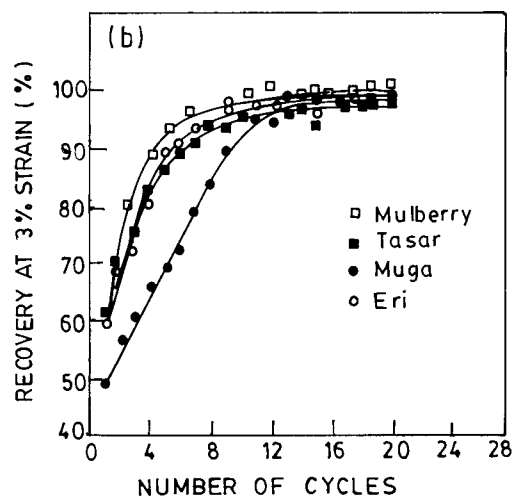
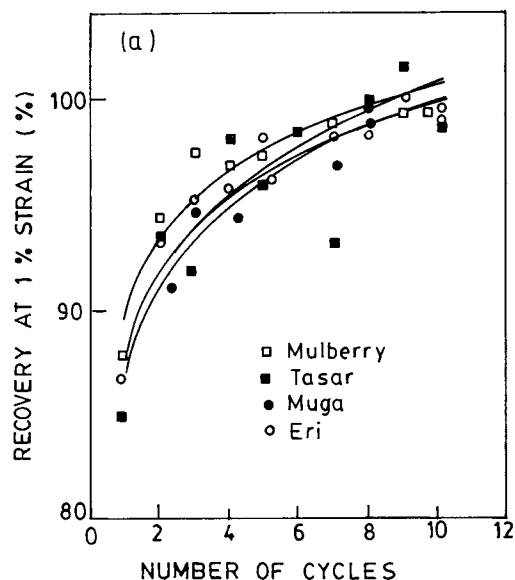


**Figure 7** Percentage recovery vs number of cycles (a) 1% strain and (b) 3% strain.

It is noteworthy that Mulberry silk fiber shows less delayed recovery, as would be expected from a fiber with lower degree of viscoelasticity. The data on total recovery (as defined in Fig. 1) is shown in Figure 11. It is noteworthy that Mulberry silk fiber, which shows the highest immediate recovery, also shows the highest total recovery. This is characteristic of an elastic fiber.

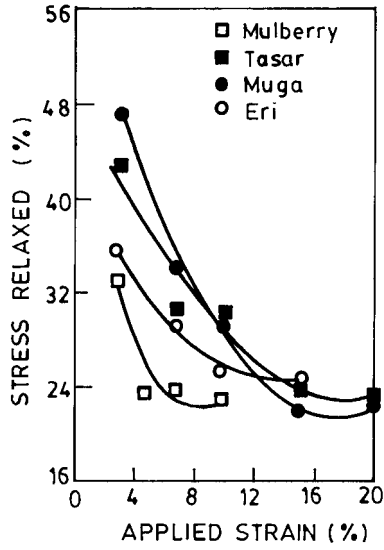


**Figure 8** Two minute stress recovery as a function of applied strain.

**Fiber Smoothness and Luster**

As seen in the earlier publication,<sup>27</sup> Eri silk fiber has a smooth surface like Mulberry silk fiber, though unlike the latter, it is not as lustrous. This may be due to the presence of a small number of large microvoids in the Eri silk fiber as lustre of silk is believed to arise from the presence of large number of small microvoids that can produce reflection and interference of light.<sup>2,20</sup>

**CONCLUSIONS**

The stress-strain behaviour of Mulberry silk fiber is strikingly different compared to that of non-

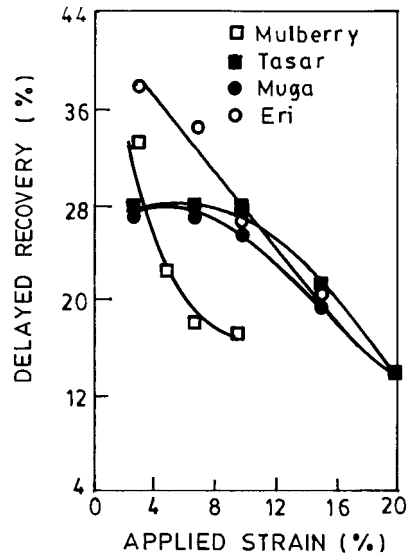


**Figure 10** Delayed recovery as a function of applied strain.

Mulberry silk fibers. All non-Mulberry silk fibers show distinct yielding, which is absent in Mulberry silk fiber. Compared to the coarser silk fibers, the finer silk fibers have higher strength and higher modulus, but lower percentage elongation-at-break; these correlate with their higher density and birefringence. Recovery characteristics of Mulberry silk fiber are superior, apparently due to its more compact structure and higher molecular order, which gives it character-

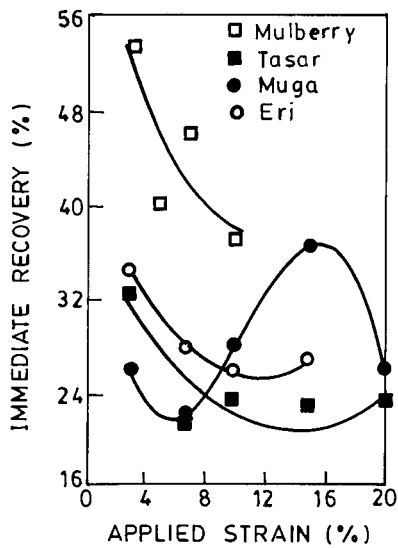


**Figure 9** Immediate recovery as a function of applied strain.

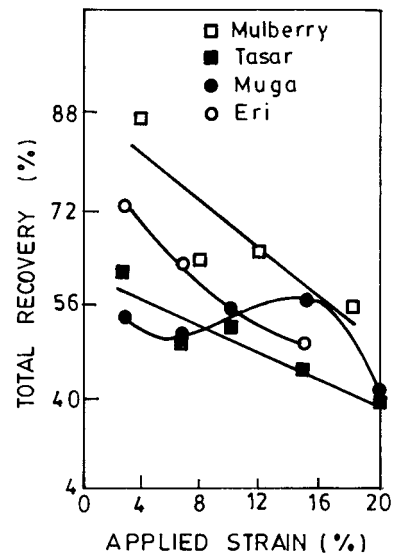


**Figure 11** Total recovery as a function of applied strain.

istics of an elastic rather than a viscoelastic fiber. Eri silk fiber, which is the most viscoelastic of the four silk fibers, has poor strength and low modulus; it also shows very distinct yield behavior.

## REFERENCES

- Gulrajani, M. L.; Sen, K.; Chattopadhyay, R. A Report, Studies in Reeling of Tasar, Department of Textile Technology, Indian Institute of Technology, Delhi, 1996.
- Iizuka, E.; Okachi, Y.; Shimizu, M.; Fukuda, A.; Hashizume, M. *Ind J Seric* 1993, 32(2), 175.
- Iizuka, E.; Okachi, Y.; Ohabayashi, S.; Fukuda, A.; Shimizu, M. *J Seric* 1993, 1(1), 1.
- Iizuka, E.; Kawano, R.; Kitani, Y.; Okachi, Y.; Shimizu, M.; Fukuda, A. *Ind J Seric* 1993, 32(1), 27.
- Iizuka, E. *J Appl Polym Sci Appl Polym Symp* 1985, 41, 173.
- Iizuka, E.; Teramoto, A.; Qun, L.; Si-Sia, M.; Shimizu, O. *J Seric Sci Jpn* 1996, 65(2), 134.
- Iizuka, E. *Int J Wild Silk Moth Silk* 1994, 1(2), 143.
- Iizuka, E. *J Seric Sci Jpn* 1995, 65(2), 102.
- Sonwalkar, T. N.; Roy, S.; Vasumathi, B. V.; Hariraj, G. *Ind J Seric* 1989, 28(2), 159.
- Das, S. Ph.D. thesis, Department of Textile Technology, Indian Institute of Technology, Delhi, 1996.
- Freddi, G.; Gotoh, Y.; Mori, T.; Tsutsui, I.; Tsukada, M. *J Appl Polym Sci* 1994, 52, 775.
- Padhi, R. C.; Labischinski, H.; Patel, A. *Polym Sci Polym Chem Ed* 1983, 21, 2863.
- Ward, I. M.; Wilding, M. A.; Brody, H. *J Polym Sci Polym Phys Ed* 1976, 14, 263.
- Gupta, V. B.; Ramesh, C.; Gupta, A. K. *J Appl Polym Sci* 1984, 29, 3115.
- Nadiger, G. S.; Bhat, N. V.; Padhye, M. R. *J Appl Polym Sci* 1985, 30, 221.
- Shaw, J. T. B.; Smith, S. G. *Biochem Biophys Acta* 1961, 52, 305.
- Kawahara, Y.; Shioya, M.; Kikutani, T.; Takaku, A. *Sen-I Gakkaishi* 1994, 50, 199.
- Bhat, N. V.; Nadiger, G. S. *J Appl Polym Sci* 1980, 25, 921.
- Tsukada, M.; Freddi, G.; Nagura, M.; Ishikawa, H.; Kasai, N. *J Appl Polym Sci* 1992, 46, 1945.
- Iizuka, E.; Uegaki, K.; Tamamatsu, H.; Okachi, Y.; Kawai, E. *J Seric Sci Jpn* 1994, 63(1), 64.
- Iizuka, E. *J Seric Sci Jpn* 1995, 65(2), 102.
- Robson, R. M. In *Handbook of Fiber Chemistry*, 2nd ed.; Lewin, M.; Pearce, E. M., Eds.; Marcel Dekker: New York, 1998; p. 446.
- Kothari, V. K.; Gupta, V. B.; Rajkhowa, R. *J Appl Polym Sci*, in press.
- Gupta, V. B.; Rana, S. K. *J Macromol Sci Phys B* 1998, 37(6), 783.
- Meredith, R. *J Text Inst* 1945, 36, 1107.
- Iizuka, E. *Biorheology* 1966, 3, 141.
- Gupta, V. B.; Rajkhowa, R.; Kothari, V. K. *Ind J Fib Text Res*, in press.